Heliyon 8 (2022) e11016

Contents lists available at ScienceDirect

Heliyon

journal homepage: www.cell.com/heliyon

Research article

Salt-inducible kinase 1 deficiency promotes vascular remodeling in pulmonary arterial hypertension via enhancement of yes-associated protein-mediated proliferation

Jiangqin Pu [1], Feng Wang [1], Peng Ye, Xiaomin Jiang, Wenying Zhou, Yue Gu, Shaoliang Chen [*]

Department of Cardiology, Nanjing First Hospital, Nanjing Medical University, Nanjing, China

ARTICLE INFO

Keywords:
Cell proliferation
Pulmonary arterial hypertension
Vascular remodeling
SIK1
YAP

ABSTRACT

Pulmonary arterial remodeling at an early stage, including excessive proliferation and migration of smooth muscle cells, is a hallmark of pulmonary arterial hypertension (PAH). Salt-inducible kinases (SIKs) have been increasingly reported to play a key role in smooth muscle cell proliferation and phenotype switching, which may be associated with arterial remodeling. However, the potential effects of SIK1 in PAH and the underlying mechanisms have not been explored. The aim of this study was to determine whether reduced expression or inactivation of SIK1 is associated with pulmonary arterial remodeling in PAH and to elucidate whether it is related to the Hippo/Yes-associated protein (YAP) pathway. Using mouse models of PAH and hypoxia-stimulated hPASMCs, we observed that SIK1 expression was robustly reduced in lung tissues of PAH mice and hPASMCs cultured under hypoxia. In hypoxia-induced PAH mice, pharmacological SIK inhibition or AAV9-mediated specific smooth muscle SIK1 knockdown strongly aggravated pathological changes caused by hypoxia, including right ventricular hypertrophy and small pulmonary arterial remodeling. Meanwhile, in hypoxia-stimulated hPASMCs, SIK1 knockdown or inhibition promoted proliferation and migration under hypoxia, accompanied by decreased phosphorylation and increased nuclear accumulation of YAP, while SIK1 overexpression inhibited hypoxia-induced proliferation, migration and nuclear translocation of YAP in hPASMCs. YAP knockdown attenuated the increase in cell proliferation induced by HG-9-91-01 treatment or SIK1 siRNA transfection under hypoxia in hPASMCs. Here, we identified SIK1 as an antiproliferative factor in hypoxia-induced pulmonary arterial remodeling via YAP-mediated mechanisms. These results show that targeting SIK1 may be a promising therapeutic strategy for the treatment of PAH.

1. Introduction

Pulmonary arterial hypertension (PAH) is a life-limiting disease characterized by vascular remodeling of the distal pulmonary arteries, which leads to a progressive increase in pulmonary vascular resistance (PVR) and heart failure [1]. Remodeling of pulmonary arteries, which results from human pulmonary arterial smooth muscle cells (PASMCs) impaired apoptosis and increased proliferation, involves obliteration of distal pulmonary arterioles, concentric pulmonary arterial wall thickening, muscularization of peripheral arteries and formation of plexiform lesions. Arterial remodeling at an early stage is believed to represent an important pathophysiological step between PAH and PVR [2,3].

The molecular pathomechanisms of pulmonary arterial remodeling in PAH are not yet completely clear. Recently, the Hippo/Yes-associated protein (YAP) pathway was shown to be involved in pulmonary arterial remodeling as a key target for hypoxia-induced cell proliferation and remodeling phenotypes [4, 5, 6]. Hippo/YAP signaling, first discovered in Drosophila melanogaster, is an ancient and evolutionarily conserved pathway that controls organ size by regulating cell survival, proliferation and apoptosis [7,8]. Core components of Hippo signaling include a kinase cascade, MST1/2 and LATS1/2, and downstream key transcriptional coactivators, Yes-associated protein (YAP) and WW domain–containing transcription regulator protein 1 (TAZ). When the Hippo pathway is activated, YAP/TAZ is phosphorylated by LATS1/2, which is

* Corresponding author.
E-mail address: chmengx@126.com (S. Chen).
[1] Equally contributing authors.

https://doi.org/10.1016/j.heliyon.2022.e11016
Received 18 February 2022; Received in revised form 29 April 2022; Accepted 5 October 2022

phosphorylated by the upstream kinases MST1/2 and sequestered in the cytoplasm [9, 10, 11, 12]. Recent studies have revealed the vital role of the Hippo/YAP pathway in the pathogenesis of PAH. In PAH PASMCs and MCT-induced PAH rats, hypoxia increased protein expression, accompanied by enhanced nuclear accumulation of YAP/TAZ and decreased YAP phosphorylation [4,5]. Knockdown of YAP in PASMCs robustly reduced proliferation and promoted apoptosis [4]. Additionally, Hippo/YAP signaling is reported to be involved in regulating cellular remodeling behaviors such as proliferative capacity, force generation and cellular motility, which are required for PAH development [6].

Salt-inducible kinases (SIKs), consisting of SIK1, SIK2 and SIK3 [13], belong to the AMP-activated protein kinase (AMPK) family of serine/threonine kinases. Recently, SIK isoforms have been shown to play a vital role in multiple pathological processes of cardiovascular diseases, including blood pressure [14,15], arterial restenosis [16] and vascular calcification [17]. In a murine model of femoral artery wire injury, SIK inhibition reduced neointima formation by suppressing VSMC proliferation and migration via SIK2-mediated AKT and PKA-CREB signaling [16]. In a murine ex vivo aortic calcification model, pharmacologic inhibition of SIKs induced histone deacetylase 4 (HDAC4) translocation and restrained vascular calcification [17]. SIK1, first found in adrenocortical tissues from high salt diet-treated rats [18], is involved in cell proliferation, migration and invasion in metabolic homeostasis and tumorigenesis [19,20]. The role of SIK1 in pulmonary arterial hypertension remains poorly understood, but several lines of evidence implicate potential relevance within PAH etiology. SIK1 activity in VSMCs has been shown to be associated with blood pressure modulation and VSMC function [14, 15, 21]. Deficiency of SIK1 triggers an increase in blood pressure by regulating NA^+, K^+-ATPase activity and associated sympathetic nervous system overdrive in *Sik1*$^{-/-}$ mice on a high-salt intake [14]. In addition, vascular SIK1 activation is crucial to the regulation of collagen in aortic adventitial fibroblasts and phenotype switching of VSMCs via TGFβ1 signaling [15]. A previous study revealed that SIK2 and SIK3 are involved in systemic growth control as Hippo/YAP pathway regulators in Drosophila [22], indicating a potential role of Hippo/YAP signaling in SIK-mediated pathogenesis. However, it is unclear whether SIK1 participates in the development of PAH and whether Hippo/YAP signaling is involved. Here, we investigated PAH mouse models and hPASMCs cultured under hypoxia to explore the role of SIKs in Hippo/-YAP signaling in mediating VSMC proliferation and migration, which results in vascular remodeling in PAH.

2. Materials and methods

2.1. Animal models of PAH

All animal procedures and protocols were approved by the Institutional Animal Care and Use Committee (IACUC) of Nanjing Medical University. Eight-week-old male wild-type (WT) C57/BL6 mice (20–25 g) were obtained from the Animal Core Facility of Nanjing Medical University. All the animals were raised at room temperature (25 °C ± 2 °C) on a 12-h light and 12-h dark cycle with access to food and ad libitum water. To establish murine PAH models, eight-week-old C57/BL6 mice were exposed to chronic hypoxia (10%) and given a subcutaneous injection of 20 mg/kg Sugen 5416 (SU5416) dissolved in dimethyl sulfoxide (DMSO) weekly for 4 weeks [23]. Control mice were kept in normoxia with weekly subcutaneous injection of PBS.

For the SIK1 inhibition (HG-9-91-01) experiment, mice were randomly divided into 3 groups (n = 13): the normoxia control group, hypoxia group and hypoxia + HG-9-91-01 group. Mice received an intraperitoneal injection of HG-9-91-01 (10 mg/kg) or vehicle (phosphate-buffered saline, PBS) every other day and were raised in normoxic (21% O_2) or hypoxic (10% O_2) chambers for 4 weeks. For the SIK1 knockdown experiment, mice were randomly divided into 3 groups (n = 13): the normoxia control group, hypoxia group and hypoxia + AAV9-SIK1-RNAi group. Mice received tail vein injection of recombinant adenoassociated virus 9 (AAV9) with a SM22α promotor (10 [10] vg in 50 μL of saline/mouse) or custom-made adenoviral vector (10 [10] vg in 50 μL of saline/mouse). Two weeks after injection, mice were raised in normoxic (21% O_2) or hypoxic (10% O_2) chambers for 4 weeks. AAV9-SM22ap-shSIK1 (CCACUUUGCUGCCAUUUAUTT) or custom-made adenoviral vector were synthesized by GeneChem (China).

2.2. Reagents and antibodies

Antibodies against YAP (sc-271134), SIK2 (sc-393139), and SIK3 (sc-515408) were purchased from Santa Cruz Biotechnology (Santa Cruz, CA, USA). Antibodies against phosphoYAP (Ser127) (#13008), LATS1 (#3477), and MST1 (#3682) were purchased from Cell Signaling Technology (Beverly, MA, USA). Antibodies against SIK1 (51045-1-AP), αSMA (14395-1-AP) and PCNA (10205-2-AP) were purchased from Proteintech (Wuhan, China). Antibodies against Ki67 (ab16667) and Cleaved-Caspase 3 (ab2302) were purchased from Abcam (Cambridge, MA, USA). The SIK inhibitor HG-9-91-01 (HY-15776) was purchased from MedChemExpress (MCE, Monmouth Junction, NJ, USA).

2.3. Cell culture and transfection

Primary human pulmonary arterial smooth muscle cells (hPASMCs, c-12521) were purchased from American Type Culture Collection (Rockville, MD, USA) and cultured in Dulbecco's Modified Eagle's Medium (DMEM, 1101, ScienCell) supplemented with 2.5% fetal bovine serum (FBS), 1% penicillin/streptomycin (PS) solution and 1% smooth muscle cell growth supplement (SMCGS). All cells were grown at 37 °C in humidified air with 5% CO_2. Cells at passages 3–9 were used for the experiments.

For hypoxia (3% O_2) experiments, hPASMCs were cultured in serum-free DMEM for 12 h before treatments and then placed in a Heracell Vios 150i CO_2 incubator (Thermo Fisher Scientific) for 24 h. For the normoxia control, hPASMCs were cultured in normal incubators with 21% O_2 for 24 h.

Transfections were performed using Lipofectamine® 3000 Transfection Reagent (L3000075, Invitrogen, CA, USA) according to the manufacturers' instructions. Short-interfering RNAs targeting SIK1 (SIK1 siRNA) (sense: 5′-CCACUUUGCUGCCAUUUAUTT-3′, antisense: 5′-AUAAAUGGCAGCAAAGUGGTT-3′) and a relative scrambled siRNA were designed and synthesized by GenePharma (China). Human YAP siRNA (sc-38637) was purchased from Santa Cruz Biotechnology. SIK1 adenovirus (Ad SIK1) and null adenovirus (Ad null) were purchased from GeneChem (China). Ad SIK1 was used to overexpress SIK1.

2.4. Western blotting

Animal tissue or whole cell lysates were harvested and lysed with radioimmunoprecipitation assay (RIPA) buffer (89900, Thermo Fisher Scientific) containing protease inhibitors and phosphatase inhibitors. Lysates were normalized using a bicinchoninic acid (BCA) protein assay kit (23227, Thermo Fisher Scientific). Equal amounts of denatured cell lysates were separated by 8% sodium dodecyl sulfate-polyacrylamide gel electrophoreses (SDS-PAGE) and then blotted onto polyvinylidene fluoride (PVDF) membranes. The blots were blocked with 5% nonfat milk for 2 h, detected with the corresponding primary antibodies overnight at 4 °C and eventually probed with appropriate secondary antibodies for 2 h at room temperature. Immunoreactivity was visualized with chemiluminescence using a Syngene Bio Imaging Device (Syngene, Cambridge, UK).

2.5. Quantitative PCR (qPCR)

Total RNA was extracted from hPASMCs using TRIzol reagent (15596026, Thermo Fisher Scientific). Reverse transcription and cDNA synthesis were performed using PrimeScript RT Master Mix (RR036A,

TaKaRa) according to the manufacturer's instructions. cDNA was amplified using SYBR Premix Ex Taq II (Tli RNaseH Plus) (RR820A, TaKaRa) in Applied Biosystems 7500 Fast RT PCR System. GAPDH was used as the internal control and the relative amount of mRNA was calculated using the comparative Ct (ΔΔCT) method.

The primer sequences were used as follows: SIK1, 5′-TTCTCCGCACACAGCTACAC-3′ (forward) and 5′-GGCATTCCGATACTCCTTGA-3′ (reverse); SIK2, 5′-GGGTGGGGTTCTACGACATC-3′ (forward) and 5′-TATTGCCACCTCCGTCTTGG-3′ (reverse); SIK3, 5′-CTCAGCCATCTCCACCTCTTCA-3′ (forward) and 5′-GGCTGCCTGAAGAGATGGTTGT-3′ (reverse); GAPDH, 5′-AGAAGGCTGGGGCTCATTTG-3′ (forward) and 5′-AGGGGCCATCCACAGTCTTC-3′ (reverse).

2.6. Immunofluorescence

Treated hPASMCs and frozen isolated sections were fixed in 4% paraformaldehyde for 30 min, blocked with 5% bovine serum albumin (BSA) for 2 h at room temperature, and then incubated overnight at 4 °C with the following primary antibodies: antiSIK1 (dilution 1:50; Proteintech), antiYAP (dilution 1:50, Santa Cruz), antiα-SMA (dilution 1:200, Proteintech), and antiKi67 (dilution 1:200, Abcam). After several washes in PBS, the cells and sections were incubated with the following appropriate directly conjugated fluorescent secondary antibodies: fluorescein isothiocyanate (FITC)-conjugated goat antimouse immunoglobulin G (IgG) (H + L) (dilution 1:200, Servicebio), Cy3-conjugated donkey antirabbit IgG (H + L) (dilution 1:200, Servicebio) for 2 h at room temperature, and diamidino-2-phenylindole (DAPI) (dilution 1:50; Beyotime) according to the manufacturer's instructions. Images were visualized by laser scanning confocal microscopy (LSM 800; Carl Zeiss, Germany).

2.7. Immunohistochemistry

Paraffin lung sections were dewaxed, placed in 10% citrate buffer, microwaved for 5 min at 180 °C, cooled at room temperature for 10 min for antigen recovery and incubated in 3% hydrogen peroxide for 20 min. The UltraVision Quanto Detection System HRP DAB Kit (Thermo Fisher Scientific) was used for the next steps according to the manufacturer's instructions. After blocking, sections were incubated separately with anti-α-SMA (1:500, Proteintech), anti-PCNA (1:500, Proteintech), and anti-Cleaved Caspase-3 (1:200, Abcam) overnight at 4 °C. Then, biotinylated secondary antibodies and peroxidase complexes were treated with 3,3′-diaminobenzidine, the peroxidase substrate, for 5 min. Antibody binding was detected using diaminobenzidine.

2.8. Hematoxylin and eosin staining

The obtained lung samples were fixed with 4% paraformaldehyde for 24 h at room temperature, embedded into paraffin, sliced into 5-μm-thick sections and stained with hematoxylin and eosin (HE). Small distal pulmonary arteries with a diameter of 50–150 μm from each slice were randomly selected for morphological analysis (20 arteries per mouse). The pulmonary artery wall thickness ratio (WT%) and pulmonary artery wall area ratio (WA%) were calculated as two indicators that determine the extent of pulmonary arterial remodeling: WT% = (outer diameter-inner diameter)/(outer diameter) × 100%; WA% = (medial wall area)/(total vessel area) × 100%.

2.9. Measurement of right ventricular systolic pressure (RVSP) and right ventricular hypertrophy index (RVHI)

After 4 weeks of normoxia or hypoxia treatment, all surviving mice were anesthetized by intraperitoneal injection of 45 mg/kg pentobarbital sodium. RVSP was measured by right heart catheterization and recorded on a Grass polygraph (Power Lab, Australia). After hemodynamic measurement, the dehydrated lungs and hearts were collected. The right ventricle (RV) was separated from the left ventricle (LV) and septum (S) in dissected mouse hearts. The right ventricular hypertrophy index (RVHI) was calculated as the ratio of RV and LV + S (RVHI = RV/[LV + S]) in each chamber.

2.10. Wound-healing assay

A wound-healing assay was used to determine the migration ability of hPASMCs. hPASMCs were plated in 35-mm diameter six-well plates. After forming a confluent monolayer, the cell layers were wounded with

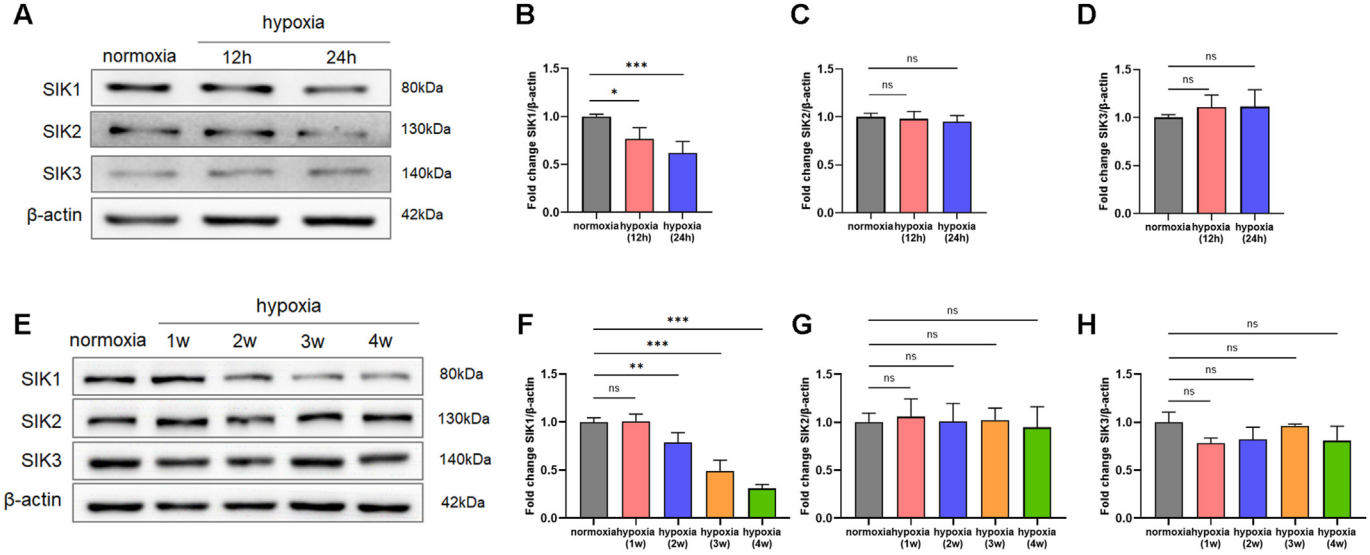

Figure 1. SIK1 levels were decreased in hypoxia-stimulated PASMCs and PAH model mice. hPASMCs were cultured under normoxia (21% O_2) or hypoxia (3% O_2) for 24 h. Male C57/BL6 mice were raised in normoxic (21% O_2) or hypoxic (10% O_2) chambers and given a subcutaneous injection of 20 mg/kg Sugen 5416 (SU5416) dissolved in DMSO weekly for 4 weeks. (A–D) Western blot analysis of SIK1, SIK2 and SIK3 protein expression in hPASMCs stimulated with hypoxia or cultured under normoxia at multiple time points (n = 4). (E–H) Western blot analysis of SIK1, SIK2 and SIK3 protein expression in lung tissues of hypoxia-induced PAH mice and normoxia control mice at weeks 1–4 (n = 4). The original blots were shown in the supplementary material (Figure SM1). Quantification of the proteins is shown in the bar graphs. Data were normalized to β-actin. All values are presented as the mean ± SD; *$p < 0.05$, **$p < 0.01$, ***$p < 0.005$; NS, no significance.

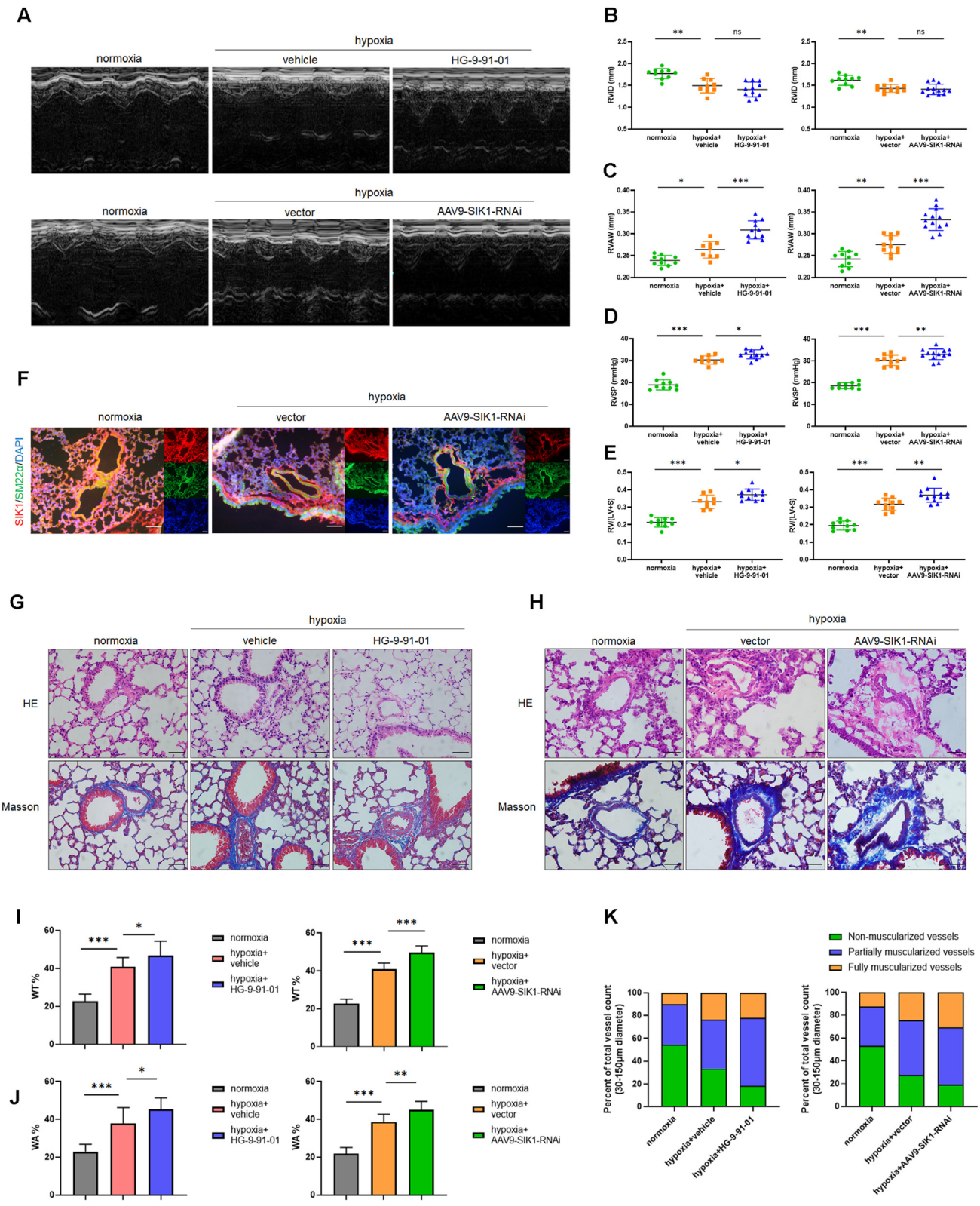

Figure 2. SIKs inhibition or specific smooth muscle SIK1 knockdown aggravated PAH development in hypoxia-induced PAH mice. (A) Representative M-mode echocardiography images of the right ventricle (RV). (B and C) Assessment of right ventricle internal diameter (RVID) and thickness of right ventricle anterior wall (RVAW) (n = 9–13). (D and E) Assessment of the mean right ventricular systolic pressure (RVSP) and RV/(LV + S) ratio (n = 9–13). (F) Representative immunofluorescence images of SIK1 (red) and α-SMA (green) in the pulmonary arteries. Scale bars = 100 μm. (G and H) Representative hematoxylin and eosin staining and Masson staining images of distal pulmonary arteries. Scale bars = 50 μm. (I–K) Assessment of the distal pulmonary artery wall thickness ratio (WT%), pulmonary artery wall area ratio (WA%) and muscularization based on HE and Masson staining (n = 9–13). All values are presented as the mean ± SD; $*p < 0.05$, $**p < 0.01$, $***p < 0.005$; NS, no significance.

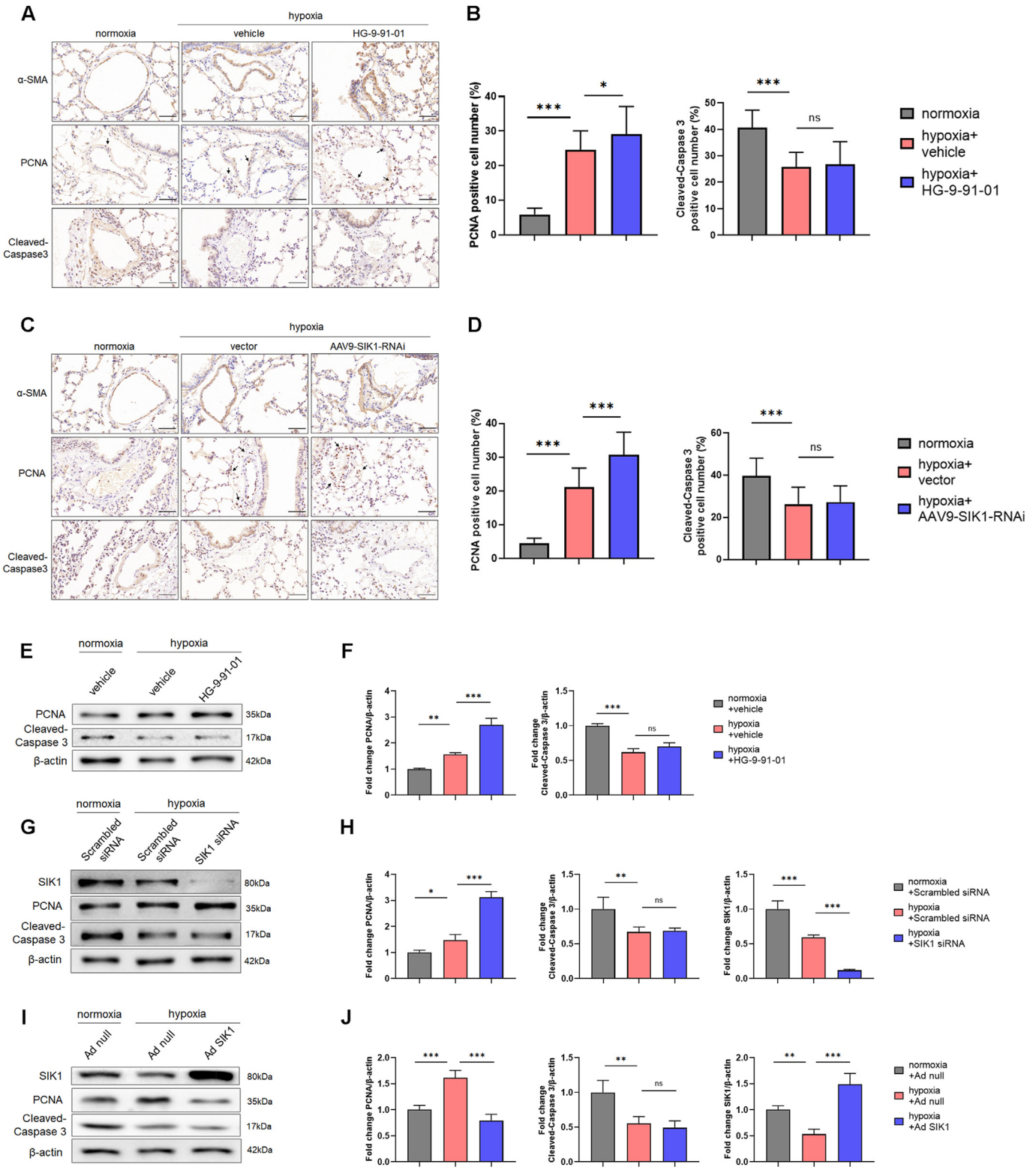

Figure 3. The effect of SIK1 on the proliferation and apoptosis of hypoxia-stimulated hPASMCs and hypoxia-induced PAH mice. (A, C) Representative immunohistochemistry images showing the expression of α-SMA (an SMC marker), proliferating cell nuclear antigen (PCNA, an indicator of proliferation) and Cleaved-Caspase3 (an indicator of apoptosis). Scale bars = 50 μm. (B, D) Quantitative analysis of the percentage of PCNA-positive and Cleaved-Caspase 3-positive PASMCs in each group (n = 20). (E and F) Western blot analysis of PCNA and Cleaved-Caspase 3 in hPASMCs treated with HG-9-91-01 or vehicle under normoxia or hypoxia (n = 4). (G and H) Western blot analysis of PCNA, Cleaved-Caspase 3 and SIK1 in hPASMCs transfected with different siRNAs under normoxia or hypoxia (n = 4). (I and J) Western blot analysis of PCNA, Cleaved-Caspase 3 and SIK1 in hPASMCs transfected with Ad SIK1 or Ad null under normoxia or hypoxia (n = 4). The original blots were shown in the supplementary material (Figure SM2). Data were normalized to β-actin. All values are presented as the mean ± SD; $*p < 0.05$, $**p < 0.01$, $***p < 0.005$; NS, no significance.

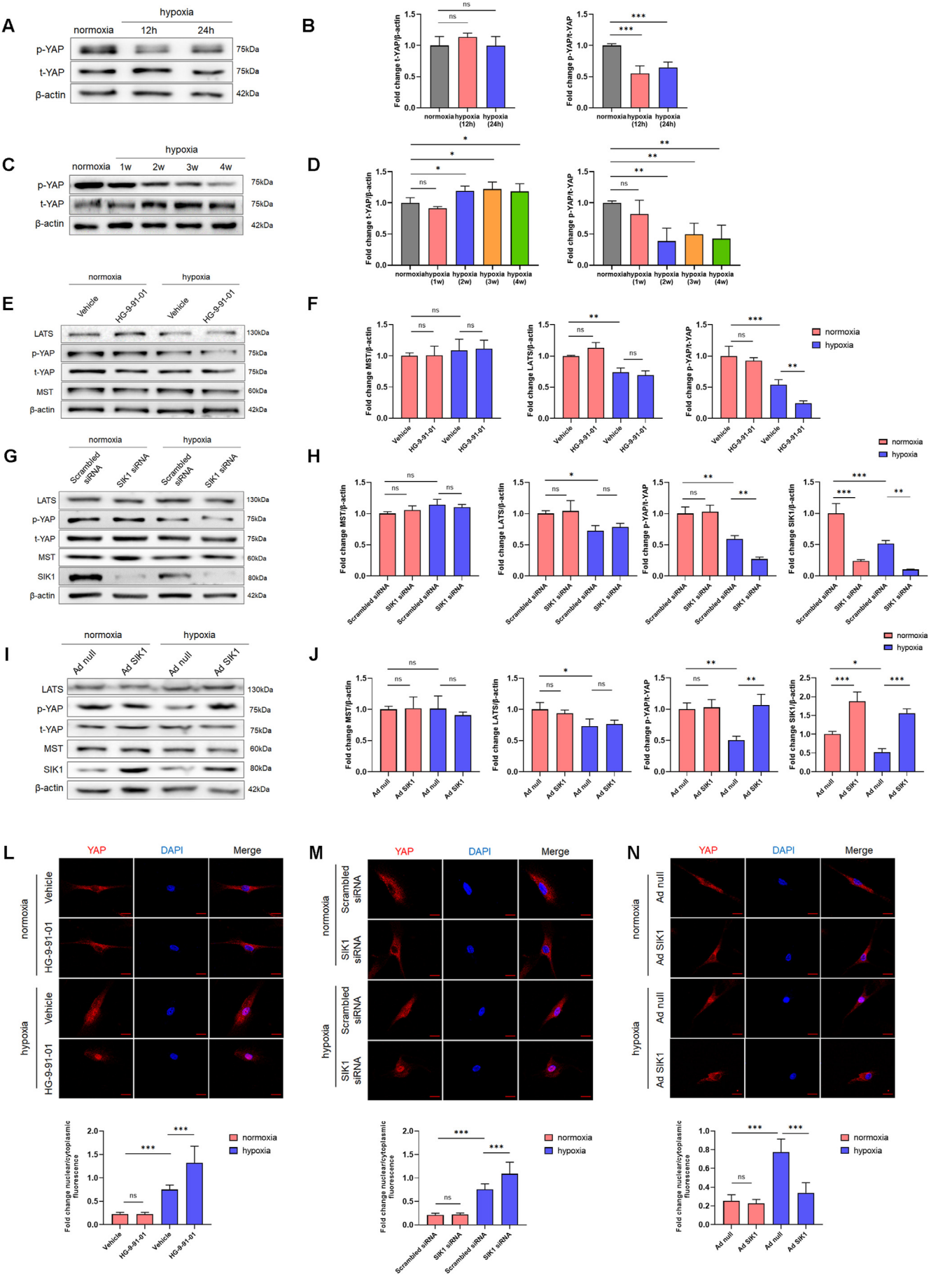

(caption on next page)

a sterile 1-ml pipette tip to obtain a noncellular area, and cell debris was washed with PBS. The medium was then replaced with fresh serum-free DMEM for 24 h. Finally, the wounded areas were observed and photographed at 0 h and 24 h, and measurements were obtained using ImageJ. Every experiment was repeated three times independently.

2.11. Statistical analysis

Quantitative data are presented as the mean ± standard deviation (SD) and were analyzed in GraphPad Prism 9.0. One-way analysis of variance (ANOVA) followed by Tukey's multiple tests were used to analyze data from multiple groups. Student's unpaired *t*-test was used to analyze data from two groups. $p < 0.05$ was considered statistically significant.

3. Results

3.1. SIK1 levels were decreased in hypoxia-stimulated PASMCs and PAH model mice

To determine the possible role of SIKs in hypoxia-induced PAH, hPASMCs were cultured under normoxia (21% O_2) or hypoxia (3% O_2) for 24 h. The results showed that hPASMC exposure to hypoxia induced a robust decrease in the protein and mRNA expression of SIK1 but not other SIK family members (Figure 1A–D, Supplementary Figure 1).

Male C57/BL6 mice were raised in normoxic (21% O_2) or hypoxic (10% O_2) chambers and given a subcutaneous injection of 20 mg/kg Sugen 5416 (SU5416) dissolved in DMSO weekly for 4 weeks. We detected the levels of SIK1, SIK2 and SIK3 in lung tissue homogenates from mice in a hypoxic chamber at weeks 1–4. Consistent with findings in hPASMCs, we observed a substantial decrease in SIK1 expression in PAH mouse lungs with prolonged hypoxia (Figure 1E–H). These findings suggest that SIK1 may be involved in PAH pathogenesis.

3.2. Pharmacological SIK1 inhibition or specific smooth muscle SIK1 knockdown aggravated PAH development in murine PAH models

To further explore whether reducing SIK1 contributed to PAH development, C57/BL6 mice received an intraperitoneal injection of the SIK inhibitor HG-9-91-01 (10 mg/kg/day) (HG-9-91-01 group) or the same volume of normal saline (vehicle group) and were raised in normoxic (21% O_2) or hypoxic (10% O_2) chambers for 4 weeks. Echocardiography was performed to evaluate right ventricular function. After 4 weeks of exposure to hypoxia, a decreased right ventricle internal diameter (RVID) (0.84-fold) and increased thickness of the right ventricle anterior wall (RVAW) (1.11-fold), mean RVSP (1.60-fold) and RV/(LV + S) ratio (1.56-fold) were observed in the vehicle group compared with the normoxia group. Mice injected with HG-9-91-01 exhibited worse RV hypertrophy than vehicle group mice over a 4-week period of hypoxia (Figure 2A–E). To further determine the role of SIK1, C57/BL6 mice were then injected with recombinant adenoassociated virus 9 with a SM22α promotor to achieve smooth muscle-specific SIK1 knockdown (AAV9-SIK1-RNAi group) or custom-made adenoviral vector (vector group) via the lateral tail vein. Smooth muscle-specific SIK1 knockdown was verified by immunofluorescence (Figure 2F). Specific knockdown of SIK1 in SMCs led to a significant increase in RVAW (1.21-fold), mean RVSP (1.31-fold) and RV/(LV + S) ratio (1.16-fold) compared with the vector group under hypoxic conditions (Figure 2A–E).

To evaluate pulmonary vessel remodeling, pathological changes in vascular remodeling were assessed by hematoxylin-eosin (HE) staining and Masson's staining. The pulmonary artery wall thickness ratio (WT%), pulmonary artery wall area ratio (WA%) and distal pulmonary artery muscularization were determined based on HE staining. Hypoxia induced a significant increase in WT%, WA% and pulmonary artery muscularization (Figure 2G–K). Masson staining showed that blue-stained collagen fibers were significantly increased in hypoxia-induced PAH mice (Figure 2G and H). Both SIK inhibition and specific smooth muscle SIK1 knockdown in mice increased WT%, WA%, collagen fiber deposition and distal pulmonary artery muscularization in pulmonary vessels of PAH mice caused by 4 weeks of hypoxia (Figure 2G–K). Taken together, our results suggested that inhibition of SIKs or loss of SIK1 aggravated the development of right ventricular hypertrophy and small pulmonary vessel remodeling, as shown in advanced PAH.

3.3. SIK1 regulates proliferation of pulmonary arteries in PAH mouse models and hypoxia-stimulated hPASMCs

Excessive proliferation and apoptosis resistance in pulmonary vascular cells play a key role in pulmonary arterial remodeling in PAH [24]. We therefore investigated the potential role of SIK1 in proliferation and apoptosis in a chronic hypoxia model of PAH. Immunohistochemistry analysis of lung sections revealed increased α-SMA and PCNA (an indicator of proliferation) expression throughout the media layer in both SIKs inhibition and specific smooth muscle SIK1 knockdown mice under hypoxia, however, neither treatment had an effect on hypoxia-induced Cleaved-Caspase 3 (an indicator of apoptosis) reduction (Figure 3A–D).

To further determine the effects of SIK1 on proliferation and apoptosis resistance in vitro, we cultured hPASMCs treated with HG-9-91-01 (1 μmol/L) or transfected them with SIK1-specific small interfering RNA (SIK1 siRNA). Both HG-9-91-01 treatment and SIK1 knockdown increased PCNA expression under hypoxia, whereas no effect on hypoxia-induced Cleaved-Caspase3 decrease was observed (Figure 3E–H). Next, we cultured hPASMCs transfected with a SIK1 adenovirus (Ad SIK1) or null adenovirus (Ad null). Western blot analysis showed that SIK1 overexpression significantly attenuated hypoxia-induced PCNA increase in hPASMCs (Figure 3I and J).

These results indicate that SIK1 may regulate hPAMSCs proliferation and pulmonary arterial remodeling as an antiproliferative factor during the development of PAH.

3.4. SIK1 regulates the Hippo/YAP pathway in PAH mouse models and hypoxia-stimulated hPASMCs

Several studies suggest that YAP functions as a critical contributor to the mechanisms underlying PAH by regulating cell proliferation, migration and apoptosis [4, 5, 25, 26]. We found that the Hippo/YAP signaling pathway was activated and that phosphorylation of YAP (Ser127) was decreased under hypoxic conditions in both hPASMCs and lung tissues of PAH mice (Figure 4A–D). To further determine whether SIK1 directly or indirectly regulates Hippo/YAP signaling, hPASMCs were treated with the SIK inhibitor HG-9-91-01 (1 μmol/L) or the same volume of the appropriate vehicle (DMSO). Western blotting showed that

Figure 4. The effect of SIK1 on YAP phosphorylation in hypoxia-stimulated hPASMCs. (A and B) Western blot analysis of p-YAP (Ser127) and t-YAP in hPASMCs cultured under normoxic and hypoxic (3%) conditions at several time points (n = 4). (C and D) Western blot analysis of p-YAP (Ser127) and t-YAP in lung tissues of normoxia control mice and hypoxia-induced PAH mice at weeks 1–4 (n = 4). (E and F) Western blot analysis of p-YAP (Ser127), t-YAP, LATS and MST in hPASMCs treated with HG-9-91-01 or vehicle under normoxia or hypoxia (n = 3). (G and H) Western blot analysis of p-YAP (Ser127), t-YAP, LATS and MST in hPASMCs transfected with different siRNAs under normoxia or hypoxia (n = 3). (I and J) Western blot analysis of p-YAP (Ser127), t-YAP, LATS and MST in hPASMCs transfected with Ad SIK1 or Ad null under normoxia or hypoxia (n = 3). The original blots were shown in the supplementary material (Figure SM3). (L and M) Immunofluorescence results showing the effect of SIK1 inhibition or SIK1 knockdown on YAP translocation under normoxic or hypoxic conditions (n = 15). Scale bars = 20 μm. (N) Immunofluorescence results showing the effect of SIK1 overexpression on YAP translocation under normoxic or hypoxic conditions (n = 15). Scale bars = 20 μm. Data were normalized to β-actin. All values are presented as the mean ± SD; $*p < 0.05$, $**p < 0.01$, $***p < 0.005$; NS, no significance.

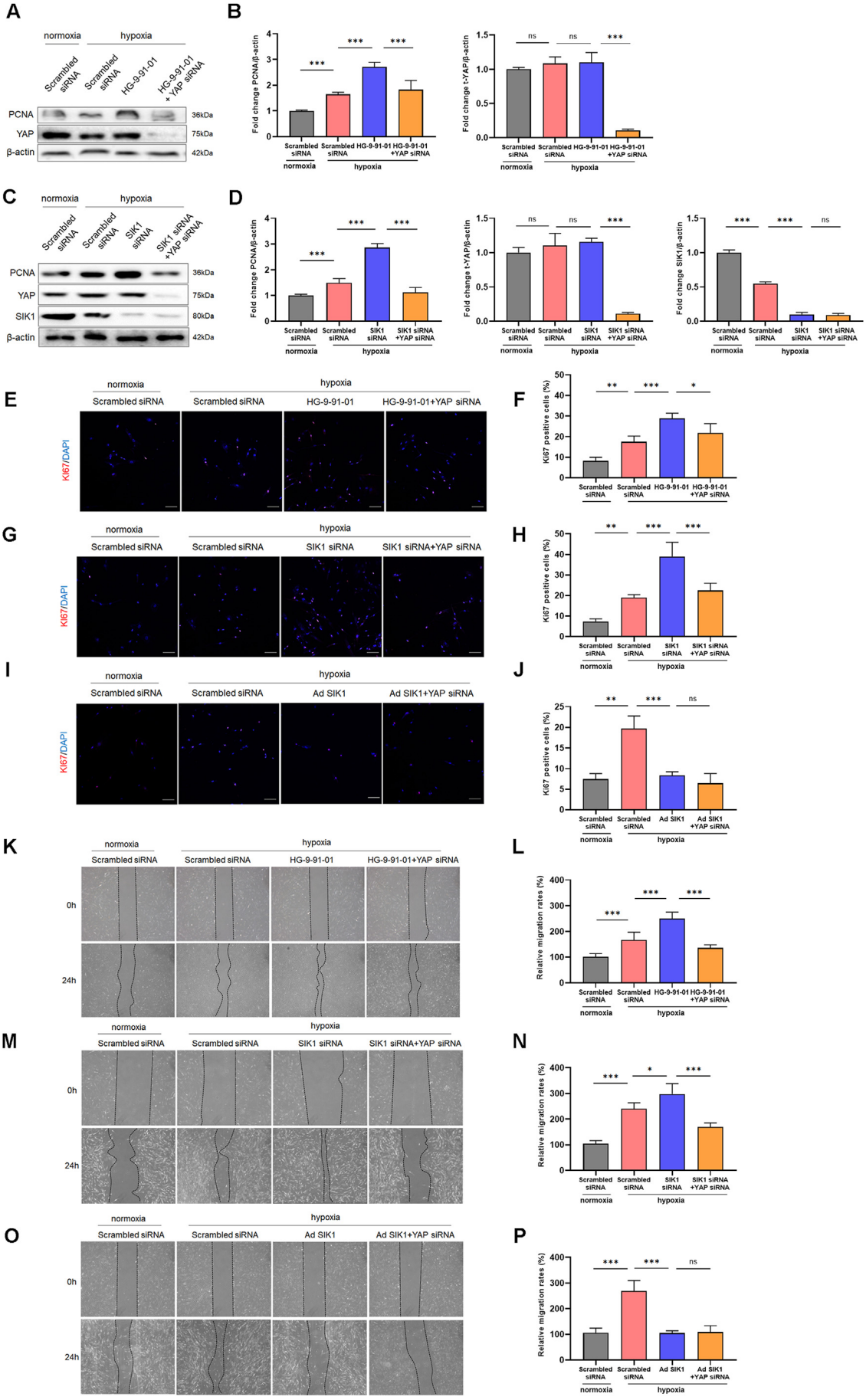

(caption on next page)

the phosphorylated YAP (Ser127)-to-YAP protein ratio was significantly decreased in the hypoxia group and markedly aggravated by HG-9-91-01 treatment. Hypoxia decreased the protein level of LATS but not MST. No significant effects of HG-9-91-01 on the expression levels of LATS and MST were observed under hypoxic conditions (Figure 4E and F). To identify the specific effects of SIK1 in hypoxia-treated hPASMCs, hPASMCs were transfected with specific SIK1 siRNA or scrambled siRNA. As expected, SIK1 siRNA specifically promoted hypoxia-induced phosphorylation reduction of YAP without alteration of t-YAP (Figure 4G and H). Then we cultured hPASMCs transfected with Ad SIK1 or Ad null. Western blot analysis showed that SIK1 overexpression dramatically inhibited hypoxia-induced phosphorylation of YAP (Figure 4I and J). Immunofluorescence staining showed that both HG-9-91-01 treatment and SIK1 siRNA transfection enhanced YAP translocation to the nucleus induced by hypoxia (Figure 4L–M), and Ad SIK1 transfection repressed hypoxia-induced nuclear translocation of YAP (Figure 4N). These data suggest that inactivation or knockdown of SIK1 decreased YAP phosphorylation and promoted YAP nuclear translocation, and that overexpression of SIK1 attenuated hypoxia-induced phosphorylation and nuclear translocation of YAP in hPASMCs.

3.5. YAP mediates the effects of SIK1 on VSMC proliferation and migration in hypoxia-stimulated PASMCs

To further determine whether SIK1 regulates the effects of YAP on VSMC proliferation and migration, we knocked down YAP in cultured hPASMCs using YAP siRNA. Both HG-9-91-01 treatment and SIK1 knockdown increased the expression of PCNA induced by hypoxia, and YAP knockdown dramatically reversed this effect on hPASMCs (Figure 5A–D). The proliferation of hPASMCs was determined by immunostaining with anti-Ki67 immunoglobulins. HG-9-91-01 treatment or SIK1 siRNA transfection promoted proliferation under hypoxia, while Ad SIK1 transfection inhibited hypoxia-induced excessive proliferation in hPASMCs. Moreover, YAP knockdown alleviated the increase in cell proliferation induced by HG-9-91-01 treatment or SIK1 siRNA transfection under hypoxia in hPASMCs (Figure 5E–J). The migration of hPASMCs was measured by wound-healing assay. Similarly, overexpression of SIK1 significantly suppressed hypoxia-induced migration in hPASMCs, and YAP knockdown attenuated hPASMC migration, which was promoted by both SIK1 inhibition and SIK1 siRNA transfection under hypoxic conditions (Figure 5K–P). Together with our findings on the role of SIK1 in YAP phosphorylation and nuclear translocation, these results suggest that the downregulation of SIK1 in PASMCs is directly related to enhanced hPASMC proliferation and migration, which is dependent on the Hippo/YAP pathway.

4. Discussion

Distal pulmonary arterial remodeling is a vital part of the pathogenesis of PAH. Hypoxia-induced vascular remodeling is critical in this complex process, including enhanced cell proliferation and migration. This study provides the first direct evidence that SIK1 is highly involved in the development of PAH by regulating YAP phosphorylation and translocation. We found that the expression of SIK1 was significantly decreased in the pulmonary arterial smooth muscle of hypoxia-induced PAH mice and hPASMCs cultured under hypoxia. SIKs inhibition or specific smooth muscle SIK1 knockdown strongly aggravated pathological changes caused by hypoxia in PAH mice, including right ventricular hypertrophy and small pulmonary arterial remodeling, via SIK1-mediated YAP phosphorylation. Meanwhile, inhibition or knockdown of SIK1 also promoted proliferation and migration in hPASMCs under hypoxia by regulating YAP phosphorylation and nuclear translocation, and overexpression of SIK1 significantly inhibited hypoxia-induced proliferation, migration and nuclear translocation of YAP in hPASMCs.

Recently, SIK1 has become a research hotspot in the fields of cell proliferation, migration and invasion. Previous studies have revealed the relevance between SIK1 deficiency and several diseases characterized by dysfunctional proliferation and metabolism. For example, down-regulated SIK1 expression was found in breast cancer [19], pancreatic cancer [20], hepatocellular carcinoma (HCC) [27], and cervical squamous cell carcinoma (CSCC) [28] and exacerbates cancer development during different periods of cancer. SIKs inhibition by HG-9-91-01 induced gluconeogenic gene expression and increased glucose production in mouse hepatocytes [29]. In line with these findings, we observed that the mRNA and protein expression level of SIK1 was decreased in hypoxia-induced PAH mice and hPASMCs cultured under hypoxia, whereas the levels of SIK2 and SIK3 changed relatively slightly with low basal expression. Pharmacological SIK1 inhibition by HG-9-91-01 or specific smooth muscle SIK1 knockdown mediated by AAV9 in PAH mice resulted in worse right ventricular hypertrophy and higher RVSP than the simple hypoxia group. All these findings indicated that SIK1 reduction was involved in PAH pathogenesis. However, the function of SIK1 in regulating PASMC behaviors and the underlying mechanisms remain to be clarified. Recent studies have reported the role of SIK1 in hypertension from the perspective of regulating vascular tone and remodeling. In VSMCs derived from human aortic arteries, the presence of the ^{15}Gly → Ser substitution within the human SIK1 protein was involved in blood pressure regulation by increasing plasma membrane NA^+, K^+-ATPase activity, which plays a vital role in vascular tone modulation. Population-based cohort analysis found that the T allele (coding for SIK1-^{15}Ser) was related to lower left ventricular mass and both lower systolic and diastolic blood pressure [21]. Loss of SIK1 induced increased collagen deposition, elevated intima/media thickness in the aorta and smooth cell phenotype switching in SIK1 knockout mice during high-salt intake via TGFβ signaling and contributed to vascular modulation and increased systolic blood pressure [15]. Additionally, CREB binding to SIK1 promoters modulates proliferation and migration in VSM cells by regulating CaMKIIδ/CREB signaling [30]. In our study, we found that SIK1 inhibition or specific smooth muscle SIK1 knockdown in hypoxia-induced PAH mice strongly aggravated pulmonary arterial remodeling, including small pulmonary arterial wall thickening and distal vascular muscularization. In hPASMCs, SIK1 overexpression by adenovirus robustly inhibited hypoxia-induced excessive cell proliferation and migration, and SIK1 inhibition by HG-9-91-01 or knockdown by siRNA promoted cell proliferation and migration under hypoxia.

Figure 5. YAP mediates the effects of SIK1 on VSMC proliferation and migration in hypoxia-stimulated PASMCs. (A and B) Western blotting analysis of PCNA and t-YAP protein expression in hPASMCs treated with HG-9-91-01 and/or YAP siRNA with or without hypoxia (n = 5). (C and D) Western blotting analysis of PCNA, t-YAP and SIK1 protein expression in hPASMCs transfected with SIK1 siRNA and/or YAP siRNA with or without hypoxia (n = 5). The original blots were shown in the supplementary material (Figure SM4). (E and F) Representative images of Ki67 (red) staining and quantitative analysis of the percentage of Ki67-positive cells in hPASMCs treated with HG-9-91-01 and/or YAP siRNA with or without hypoxia (n = 5). Scale bars = 100 μm. (G and H) Representative images of Ki67 (red) staining and quantitative analysis of the percentage of Ki67-positive cells in hPASMCs transfected with SIK1 siRNA and/or YAP siRNA with or without hypoxia (n = 5). Scale bars = 100 μm. (I and J) Representative images of Ki67 (red) staining and quantitative analysis of the percentage of Ki67-positive cells in hPASMCs transfected with Ad SIK1 and/or YAP siRNA with or without hypoxia (n = 5). Scale bars = 100 μm. (K and L) Representative images of the wound-healing assay and quantitative analysis of migrated cells in hPASMCs treated with HG-9-91-01 and/or YAP siRNA with or without hypoxia (n = 6). (M and N) Representative images of the wound-healing assay and quantitative analysis of migrated cells in hPASMCs transfected with SIK1 siRNA and/or YAP siRNA with or without hypoxia (n = 6). (O and P) Representative images of the wound-healing assay and quantitative analysis of migrated cells in hPASMCs transfected with Ad SIK1 and/or YAP siRNA with or without hypoxia (n = 6). Data were normalized to β-actin. All values are presented as the mean ± SD; $^*p < 0.05$, $^{**}p < 0.01$, $^{***}p < 0.005$; NS, no significance.

Additionally, the expression of PCNA (an indicator of proliferation) was elevated in both SIK1 inhibition or knockdown hPASMCs and lung sections of PAH mice. Our findings indicated that downregulation of SIK1 is directly related to hPASMC proliferation and migration in hPASMCs and contributes to vascular remodeling in hypoxia-induced PAH mice. Though the upstream pathway leads to the decrease of SIK1 in PAH remains unknown, emerging studies demonstrated that some cancer-like phenotypes in PAH, including Warburg metabolism, mitochondrial fragmentation, excessive proliferation and impaired apoptosis, suggested a link between pathomechanism of PAH and cancer under hypoxia [31]. Recent studies showed that several microRNAs regulated SIK1 expression post-transcriptionally in multiple cancers by targeting 3′UTR of SIK1. For example, microRNA-25 (miR-25) shuttled through CSQT-2-derived exosomes aggravated hepatocellular carcinoma (HCC) in Hep3B and Huh-7 cells [27], and miR-203 promotes cell proliferation, migration and invasion in pancreatic cancer cells [20]. These studies suggested a possible mechanism of SIK1 reduction in PAH. Nevertheless, we found that mRNA level of SIK1 decrease robustly, which consistent with alteration of protein level in hypoxia-induced hPASMCs in our study. These results indicated that SIK1 was regulated on the transcriptional level by hypoxia stimulation in hPASMCs. Further studies are essential to determine the specific mechanism of SIK1 reduction in PAH.

Another outstanding question concerns what mediated SIK1 regulation on cell proliferation and migration under hypoxia. In our vitro and in vivo experiments, we observed that the expression level of SIK1 was decreased with dysfunctional Hippo/YAP pathway signaling. In hPASMCs, YAP was primarily distributed in the cytoplasm of HPASMCs. SIK1 knockdown or inhibition led to reduced YAP phosphorylation and increased nuclear translocation, and SIK1 overexpression repressed phosphorylation and nuclear translocation of YAP under hypoxia in hPASMCs, indicating that hypoxia-induced YAP dephosphorylation and nuclear translocation were regulated by SIK1. These provocative findings strengthen the notion that SIK1/YAP represents a novel mechanism related to PAH development.

The Hippo/YAP pathway includes the upstream kinase cascade, MST1/2 and LATS1/2, and downstream effector YAP/TAZ transcription coactivators. Emerging evidence has proven that Hippo/YAP signaling mediates proliferation, migration, and apoptosis in cultured PASMCs [25, 26] and is related to pulmonary vascular remodeling in MCT-induced PAH rats [32,33]. In idiopathic PAH lungs and distal pulmonary arterial vascular smooth muscle cells from patients with idiopathic PAH, inactive Hippo/LATS1 promoted PASMC proliferative and apoptotic responses by upregulating the effector YAP [4], while deletion of YAP repressed pulmonary vascular remodeling in cardiac/SMC-specific YAP knockout mice [34]. The function of the Hippo/YAP pathway is determined by YAP localization. Once the Hippo/YAP pathway is off, dephosphorylated YAP translocates to the nucleus and interacts with TEAD family transcription factors to promote related gene expression [8, 35]. In MCT-induced PAH rats, YAP was highly expressed and dephosphorylated, accompanied by nuclear translocation of YAP [5, 32, 33]. Here, we presented evidence that SIK1 regulates hypoxia-induced pulmonary arterial remodeling by modulating YAP phosphorylation and translocation. In our study, we observed sustained reduced phosphorylation and increased nuclear accumulation of YAP in the lung tissues of hypoxia-induced PAH mouse models and hypoxia-stimulated hPASMCs, along with excessive proliferation of PASMCs and pulmonary arterial remodeling, while knockdown of YAP reversed this effect by suppressing PASMC proliferation and migration. However, the exact mechanism by which SIK1 inhibits YAP phosphorylation and promotes YAP nuclear translocation remains unclear. In our study, we found that the levels of the YAP upstream kinases MST and LATS were not affected by inhibition or knockdown of SIK1, which indicated an undiscovered molecular mechanism underlying SIK1-mediated YAP translocation. Cyclic AMP-response-element binding protein (CREB)-regulated transcriptional coactivators (CRTC1, CRTC2 and CRTC3) and Class 2a histone deacetylases (HDAC4, HDAC5, HDAC7 and HDAC9) are two main groups of substrates of SIK1 [36,37,38]. SIKs are involved in vascular calcification by controlling the cytoplasmic location and function of HDAC4 in VSMCs [17], and have an important role in stress-mediated pathologic cardiomyocyte remodeling by stabilizing HDAC7 protein [39]. Moreover, accumulating evidence indicated that HDAC inhibitors suppress YAP expression in several cancer cells, and the localization of YAP in these cells is related to resistance to HDAC inhibitor treatments [40]. Thus, we speculate that SIK1 affects YAP nuclear translocation by regulating one or more HDACs and CRTCs, however, further studies are required to confirm the related mechanisms.

Collectively, our study elucidated, for the first time to our knowledge, the key role of SIK1/YAP crosstalk in pulmonary arterial remodeling in hypoxia-induced PAH by regulating the proliferation and migration of PASMCs and provides an effective target for PAH therapeutic intervention. Our results demonstrated that SIK1 was downregulated under hypoxia as an antiproliferation factor. Inhibition or knockdown of SIK1 aggravated right ventricular hypertrophy and vascular remodeling in vivo and promoted hPASMC proliferation and migration in vitro. Reduction of YAP phosphorylation and increased YAP nuclear translocation are required for SIK1-mediated pulmonary arterial remodeling and excessive proliferation under hypoxia.

4.1. What's new

This is the first study demonstrating the antiproliferative role of SIK1 in pulmonary arterial remodeling in hypoxia-induced PAH via YAP-dependent mechanisms. SIK1 was robustly decreased in lung tissues of hypoxia-induced PAH mice and hPASMCs cultured under hypoxia. Deficiency or inactivation of SIK1 blocked the phosphorylation of YAP at serine 127 and promoted YAP nuclear accumulation, which likely contributed to the antiproliferative effects of SIK1.

4.2. Limitations

HG-9-91-01 is a pan-SIK inhibitor with IC50 values of 0.92 nM, 6.6 nM and 9.6 nM for SIK1, SIK2, and SIK3, respectively [41]. Although there was no significant alteration in the expression levels of SIK2 and SIK3 with low basal expression in hypoxia-stimulated hPASMCs in our study, a recent study reported that SIK3 has a potential role in VSMC proliferation and arterial restenosis [16], which might also be inhibited in our study. Moreover, overexpression of SIK1 in PAH mice will make our conclusion more comprehensive.

Declarations

Author contribution statement

Shaoliang Chen: Conceived and designed the experiments; Contributed reagents, materials, analysis tools or data; Analyzed and interpreted the data.

Jiangqin Pu, Feng Wang, Peng Ye and Xiaomin Jiang: Performed the experiments; Analyzed and interpreted the data; Wrote the paper.

Wenying Zhou and Yue Gu: Conceived and designed the experiments; Analyzed and interpreted the data.

Funding statement

Shaoliang Chen was supported by National Natural Science Foundation of China [91639303] and the Natural Science Foundation of Jiangsu Province [BK20191117].

Data availability statement

Data will be made available on request.

Declaration of interest's statement

The authors declare no conflict of interest.

Additional information

Supplementary content related to this article has been published online at https://doi.org/10.1016/j.heliyon.2022.e11016.

References

[1] V.V. McLaughlin, M.D. McGoon, Pulmonary arterial hypertension, Circulation 114 (2006) 1417–1431.

[2] R.M. Tuder, E. Stacher, J. Robinson, R. Kumar, B.B. Graham, Pathology of pulmonary hypertension, Clin. Chest Med. 34 (2013) 639–650.

[3] L. Calvier, P. Boucher, J. Herz, G. Hansmann, LRP1 deficiency in vascular SMC leads to pulmonary arterial hypertension that is reversed by PPARgamma activation, Circ. Res. 124 (2019) 1778–1785.

[4] T.V. Kudryashova, D.A. Goncharov, A. Pena, N. Kelly, R. Vanderpool, J. Baust, A. Kobir, W. Shufesky, A.L. Mora, A.E. Morelli, J. Zhao, K. Ihida-Stansbury, B. Chang, H. DeLisser, R.M. Tuder, S.M. Kawut, H.H. Sillje, S. Shapiro, Y. Zhao, E.A. Goncharova, HIPPO-Integrin-linked kinase cross-talk controls self-sustaining proliferation and survival in pulmonary hypertension, Am. J. Respir. Crit. Care Med. 194 (2016) 866–877.

[5] Q. Wang, W. Shi, Q. Zhang, W. Feng, J. Wang, C. Zhai, X. Yan, M. Li, Inhibition of Siah2 ubiquitin ligase ameliorates monocrotaline-induced pulmonary arterial remodeling through inactivation of YAP, Life Sci. 242 (2020), 117159.

[6] P.B. Dieffenbach, C.M. Haeger, A.M.F. Coronata, K.M. Choi, X. Varelas, D.J. Tschumperlin, L.E. Fredenburgh, Arterial stiffness induces remodeling phenotypes in pulmonary artery smooth muscle cells via YAP/TAZ-mediated repression of cyclooxygenase-2, Am. J. Physiol. Lung Cell Mol. Physiol. 313 (2017) L628–L647.

[7] K.F. Harvey, C.M. Pfleger, I.K. Hariharan, The Drosophila Mst Ortholog, hippo, Restricts growth and cell proliferation and promotes apoptosis, Cell 114 (2003) 457–467.

[8] J. Huang, S. Wu, J. Barrera, K. Matthews, D. Pan, The Hippo signaling pathway coordinately regulates cell proliferation and apoptosis by inactivating Yorkie, the Drosophila Homolog of YAP, Cell 122 (2005) 421–434.

[9] E.H. Chan, M. Nousiainen, R.B. Chalamalasetty, A. Schafer, E.A. Nigg, H.H. Sillje, The Ste20-like kinase Mst2 activates the human large tumor suppressor kinase Lats1, Oncogene 24 (2005) 2076–2086.

[10] J. Dong, G. Feldmann, J. Huang, S. Wu, N. Zhang, S.A. Comerford, M.F. Gayyed, R.A. Anders, A. Maitra, D. Pan, Elucidation of a universal size-control mechanism in Drosophila and mammals, Cell 130 (2007) 1120–1133.

[11] B. Zhao, X. Wei, W. Li, R.S. Udan, Q. Yang, J. Kim, J. Xie, T. Ikenoue, J. Yu, L. Li, P. Zheng, K. Ye, A. Chinnaiyan, G. Halder, Z.C. Lai, K.L. Guan, Inactivation of YAP oncoprotein by the Hippo pathway is involved in cell contact inhibition and tissue growth control, Genes Dev. 21 (2007) 2747–2761.

[12] F.L.D. Liu, K.M. Choi, L. Stopfer, A. Marinković, V. Vrbanac, C.K. Probst, S.E. Hiemer, T.H. Sisson, J.C. Horowitz, I.O. Rosas, L.E. Fredenburgh, C. Feghali-Bostwick, X. Varelas, A.M. Tager, D.J. Tschumperlin, Mechanosignaling through YAP and TAZ drives fibroblast activation and fibrosis, Am. J. Physiol. Lung Cell Mol. Physiol. 308 (2015) L344–L357.

[13] M. Okamoto, H. Takemori, Y. Katoh, Salt-inducible kinase in steroidogenesis and adipogenesis, Trends Endocrinol. Metabol. 15 (2004) 21–26.

[14] N.M. Pires, B. Igreja, M.P. Serrao, E.F. Matias, E. Moura, T. Antonio, F.L. Campos, L. Brion, A. Bertorello, P. Soares-da-Silva, Acute salt loading induces sympathetic nervous system overdrive in mice lacking salt-inducible kinase 1 (SIK1), Hypertens. Res. 42 (2019) 1114–1124.

[15] A.M. Bertorello, N. Pires, B. Igreja, M.J. Pinho, E. Vorkapic, D. Wagsater, J. Wikstrom, M. Behrendt, A. Hamsten, P. Eriksson, P. Soares-da-Silva, L. Brion, Increased arterial blood pressure and vascular remodeling in mice lacking salt-inducible kinase 1 (SIK1), Circ. Res. 116 (2015) 642–652.

[16] Y. Cai, X.L. Wang, J. Lu, X. Lin, J. Dong, R.J. Guzman, Salt-inducible kinase 3 promotes vascular smooth muscle cell proliferation and arterial restenosis by regulating AKT and PKA-CREB signaling, Arterioscler. Thromb. Vasc. Biol. 41 (2021) 2431–2451.

[17] A. Abend, O. Shkedi, M. Fertouk, L.H. Caspi, I. Kehat, Salt-inducible kinase induces cytoplasmic histone deacetylase 4 to promote vascular calcification, EMBO Rep. 18 (2017) 1166–1185.

[18] Z.T.H. Wang, S.K. Halder, Y. Nonaka, M. Okamoto, Cloning of a novel kinase (SIK) of the SNF1/AMPK family from high salt diet-treated rat adrenal1, FEBS Lett. 453 (1999) 135–139.

[19] L. Ponnusamy, R. Manoharan, Distinctive role of SIK1 and SIK3 isoforms in aerobic glycolysis and cell growth of breast cancer through the regulation of p53 and mTOR signaling pathways, Biochim. Biophys. Acta Mol. Cell Res. 1868 (2021), 118975.

[20] Z.G. Ren, S.X. Dong, P. Han, J. Qi, miR-203 promotes proliferation, migration and invasion by degrading SIK1 in pancreatic cancer, Oncol. Rep. 35 (2016) 1365–1374.

[21] S. Popov, A. Silveira, D. Wagsater, H. Takemori, R. Oguro, S. Matsumoto, K. Sugimoto, K. Kamide, T. Hirose, M. Satoh, H. Metoki, M. Kikuya, T. Ohkubo, T. Katsuya, H. Rakugi, Y. Imai, F. Sanchez, M. Leosdottir, A.C. Syvanen, A. Hamsten, O. Melander, A.M. Bertorello, Salt-inducible kinase 1 influences Na(+),K(+)-ATPase activity in vascular smooth muscle cells and associates with variations in blood pressure, J. Hypertens. 29 (2011) 2395–2403.

[22] M.C. Wehr, M.V. Holder, I. Gailite, R.E. Saunders, T.M. Maile, E. Ciirdaeva, R. Instrell, M. Jiang, M. Howell, M.J. Rossner, N. Tapon, Salt-inducible kinases regulate growth through the Hippo signalling pathway in Drosophila, Nat. Cell Biol. 15 (2013) 61–71.

[23] S. Provencher, S.L. Archer, F.D. Ramirez, B. Hibbert, R. Paulin, O. Boucherat, Y. Lacasse, S. Bonnet, Standards and methodological rigor in pulmonary arterial hypertension preclinical and translational research, Circ. Res. 122 (2018) 1021–1032.

[24] R. Paulin, E.D. Michelakis, The metabolic theory of pulmonary arterial hypertension, Circ. Res. 115 (2014) 148–164.

[25] W. Shi, Q. Wang, J. Wang, X. Yan, W. Feng, Q. Zhang, C. Zhai, L. Chai, S. Li, X. Xie, M. Li, Activation of yes-associated protein mediates sphingosine-1-phosphate-induced proliferation and migration of pulmonary artery smooth muscle cells and its potential mechanisms, J. Cell. Physiol. 236 (2021) 4694–4708.

[26] Q. Zhang, W. Li, Y. Zhu, Q. Wang, C. Zhai, W. Shi, W. Feng, J. Wang, X. Yan, L. Chai, Y. Chen, C. Li, P. Liu, M. Li, Activation of AMPK inhibits Galectin-3-induced pulmonary artery smooth muscle cells proliferation by upregulating hippo signaling effector YAP, Mol. Cell. Biochem. 476 (2021) 3037–3049.

[27] X. Fu, Y. Tang, W. Wu, Y. Ouyang, D. Tan, Y. Huang, Exosomal microRNA-25 released from cancer cells targets SIK1 to promote hepatocellular carcinoma tumorigenesis, Dig. Liver Dis. (2021).

[28] J. Peng, F. Hou, W. Zhu, J. Li, Z. Teng, lncRNA NR2F1-AS1 regulates miR-17/SIK1 Axis to suppress the invasion and migration of cervical squamous cell carcinoma cells, Reprod. Sci. 27 (2020) 1534–1539.

[29] K. Patel, M. Foretz, A. Marion, D.G. Campbell, R. Gourlay, N. Boudaba, E. Tournier, P. Titchenell, M. Peggie, M. Deak, M. Wan, K.H. Kaestner, O. Goransson, B. Viollet, N.S. Gray, M.J. Birnbaum, C. Sutherland, K. Sakamoto, The LKB1-salt-inducible kinase pathway functions as a key gluconeogenic suppressor in the liver, Nat. Commun. 5 (2014) 4535.

[30] Y. Liu, L.Y. Sun, D.V. Singer, R. Ginnan, H.A. Singer, CaMKIIdelta-dependent inhibition of cAMP-response element-binding protein activity in vascular smooth muscle, J. Biol. Chem. 288 (2013) 33519–33529.

[31] T. Thenappan, M.L. Ormiston, J.J. Ryan, S.L. Archer, Pulmonary arterial hypertension: pathogenesis and clinical management, BMJ 360 (2018) j5492.

[32] W. Zuo, N. Liu, Y. Zeng, Z. Xiao, K. Wu, F. Yang, B. Li, Q. Song, Y. Xiao, Q. Liu, Luteolin ameliorates experimental pulmonary arterial hypertension via suppressing hippo-YAP/PI3K/AKT signaling pathway, Front. Pharmacol. 12 (2021), 663551.

[33] D. Yan, G. Li, Y. Zhang, Y. Liu, Angiotensin-converting enzyme 2 activation suppresses pulmonary vascular remodeling by inducing apoptosis through the Hippo signaling pathway in rats with pulmonary arterial hypertension, Clin. Exp. Hypertens. 41 (2019) 589–598.

[34] Y. Wang, G. Hu, F. Liu, X. Wang, M. Wu, J.J. Schwarz, J. Zhou, Deletion of yes-associated protein (YAP) specifically in cardiac and vascular smooth muscle cells reveals a crucial role for YAP in mouse cardiovascular development, Circ. Res. 114 (2014) 957–965.

[35] Y. Mesrouze, F. Bokhovchuk, M. Meyerhofer, P. Fontana, C. Zimmermann, T. Martin, C. Delaunay, D. Erdmann, T. Schmelzle, P. Chene, Dissection of the interaction between the intrinsically disordered YAP protein and the transcription factor TEAD, Elife 6 (2017).

[36] N.J. Darling, P. Cohen, Nuts and bolts of the salt-inducible kinases (SIKs), Biochem. J. 478 (2021) 1377–1397.

[37] Y. Katoh, H. Takemori, X.Z. Lin, M. Tamura, M. Muraoka, T. Satoh, Y. Tsuchiya, L. Min, J. Doi, A. Miyauchi, L.A. Witters, H. Nakamura, M. Okamoto, Silencing the constitutive active transcription factor CREB by the LKB1-SIK signaling cascade, FEBS J. 273 (2006) 2730–2748.

[38] R. Berdeaux, N. Goebel, L. Banaszynski, H. Takemori, T. Wandless, G.D. Shelton, M. Montminy, SIK1 is a class II HDAC kinase that promotes survival of skeletal myocytes, Nat. Med. 13 (2007) 597–603.

[39] A. Hsu, Q. Duan, S. McMahon, Y. Huang, S.A. Wood, N.S. Gray, B. Wang, B.G. Bruneau, S.M. Haldar, Salt-inducible kinase 1 maintains HDAC7 stability to promote pathologic cardiac remodeling, J. Clin. Invest. 130 (2020) 2966–2977.

[40] H. Han, B. Yang, H.J. Nakaoka, J. Yang, Y. Zhao, K. Le Nguyen, A.T. Bishara, T.K. Mandalia, W. Wang, Hippo signaling dysfunction induces cancer cell addiction to YAP, Oncogene 37 (2018) 6414–6424.

[41] K. Clark, K.F. MacKenzie, K. Petkevicius, Y. Kristariyanto, J. Zhang, H.G. Choi, M. Peggie, L. Plater, P.G. Pedrioli, E. McIver, N.S. Gray, J.S. Arthur, P. Cohen, Phosphorylation of CRTC3 by the salt-inducible kinases controls the interconversion of classically activated and regulatory macrophages, Proc. Natl. Acad. Sci. U. S. A. 109 (2012) 16986–16991.